Available online at www.sciencedirect.com
SCIENCE DIRECT®
PERGAMON
International Journal of Rock Mechanics & Mining Sciences 40 (2003) 221–232
International Journal of Rock Mechanics and Mining Sciences
www.elsevier.com/locate/ijrmms

Post-failure behavior of two mine pillars confined with backfill

D.R. Tesarik[a,*], J.B. Seymour[a], T.R. Yanske[b]

[a] NIOSH-Spokane Research Laboratory, 315 E. Montgomery Avenue, Spokane, WA 99207, USA
[b] The Doe Run Company, Airport Road no. 2, Viburnum, MO 65566, USA

Accepted 1 December 2002

Abstract

Researchers from the National Institute for Occupational Safety and Health used a series of instruments (borehole extensometers, earth pressure cells, and embedment strain gauges) to study the post-failure behavior of two pillars confined by backfill in a test section at the Buick Mine near Boss, MO, USA. Evaluation of these pillars was part of a research project to assess the safety of the test section when high-grade support pillars were mined.

Data from borehole extensometers installed in several backfill-confined pillars and numerical modeling indicated that these pillars failed during extraction of the support pillars. Failure was corroborated by the post-yield pillar strain response in which the immediate elastic strain was negligible compared to the time-dependent strain component measured between blasting rounds.

A three-dimensional, finite-element program with an elastic perfectly plastic material model was calibrated using extensometer data to estimate rock mass modulus and unconfined compressive strength. The resulting rock mass modulus was 45–60% of the average deformation modulus obtained from laboratory tests, and the calibrated compressive strength was 40% of average laboratory values. A rock mass modulus equal to 52% of the average laboratory deformation modulus was calculated using the rock mass rating (RMR) system. Rock mass strength was calculated with the generalized Hoek–Brown failure criterion for jointed rock and indicated that in situ strength was 33% of laboratory strength. Post-failure stresses calculated by the finite-element model were larger for confined pillars than post-failure stresses in unconfined pillars calculated using empirical plots. Data from the calibrated model provided a strain-hardening stress-versus-strain relationship. This knowledge is critical for the design of mines that use partially failed pillars to carry overburden load.

1. Introduction

An important aspect of mine development is planning the excavation sequence so the resource can be mined safely and economically. Computer models can be useful tools for evaluating different excavation sequences and identifying zones of high stress and potential failure prior to actual mining. To achieve reasonable predictions, the model must be calibrated with in situ measurements so that average rock mass property values can be determined.

Rock mass modulus of deformation can be obtained by comparing changes between measured and model-predicted strain in rock that is presumed to be elastic during the time of measurement. Estimating rock mass strength is more difficult because instruments are not always installed in areas of the mine that will fail, failure zones are not always easily discernable through observation, and instruments or their cables are often damaged if the rock fails. Measuring post-failure stress or strain is even more difficult because the capabilities of the instruments can be exceeded, and the instruments can lose anchorage within the rock.

Knowledge of the post-failure behavior of pillars is becoming more important as the depths of mines increase [1]. The mine design process must include calculations of pillar failure, but the post-failure stress–strain relationship is often unknown [2]. The objectives of the work reviewed here were to describe the post-failure stress–strain relationship for rockfill-confined pillars in a section of the Buick Mine known as area 5 (Fig. 1) and to estimate rock mass modulus, uniaxial compressive strength, and residual strength of these pillars.

*Corresponding author. Tel.: +1-509-354-8052; fax: +1-509-354-8099.
E-mail addresses: det4@cdc.gov (D.R. Tesarik), zia8@cdc.gov (J.B. Seymour), tyankse@doerun.com (T.R. Yanske).

1365-1609/03/$ - see front matter
doi:10.1016/S1365-1609(02)00139-9

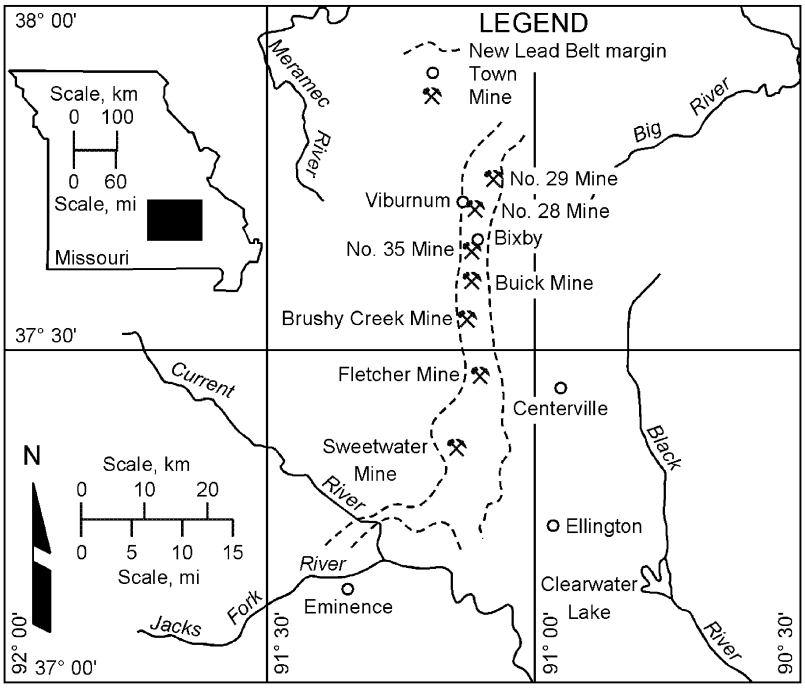

Fig. 1. Location of Buick Mine in New Lead Belt, Missouri, USA.

The Buick Mine is one of seven mines in southeast Missouri operated by The Doe Run Co., St. Louis, MO, in a deposit called the New Lead Belt or the Viburnum Trend. The deposit is a flat-lying, tabular ore body lying under 150–360 m (492–1181 ft) of overburden. The ore body is 1–40 m (3–131 ft) thick and 10–600 m (33–1969 ft) wide and has a trend length of 65 km (40 mile) (Fig. 1). In general, the deposit has two main joint sets and one set of horizontal bedding planes with discontinuities spaced from 13 cm to 2 m (5 in to 6.6 ft). One joint set trends N45°E and dips 70–90° to the southeast, and the other trends N45°W and dips 70–90° to the southwest. The host rock consists of beds of dolomite intermixed with layers of shale 5–10 m (16–33 ft) thick overlain by the soft, friable 43-m- (141-ft-) thick Davis Shale. Competent dolomite extends from the top of the Davis Shale to the weathered surface. The immediate floor is a very competent, medium-crystalline dolomite (Fig. 2).

A mechanized room-and-pillar technique is used to extract lead, zinc, and copper ore. Two-boom drill jumbos; 7- to 9-ton (8- to 10-st-) capacity loaders; and 27- to 45-ton- (30- to 50-st-) capacity haul trucks are used for primary room development. Development cuts consist of a combination of back, bottom, undercut, and overcut passes. Before backfill was used to enable the extraction of support pillars, pillars measured 9×9 m (30×30 ft) with 10.7-m- (35-ft-) wide drifts between them. Because of the success of pillar extraction in area 5, larger panel pillars measuring 11.5×23 m (38×75 ft)

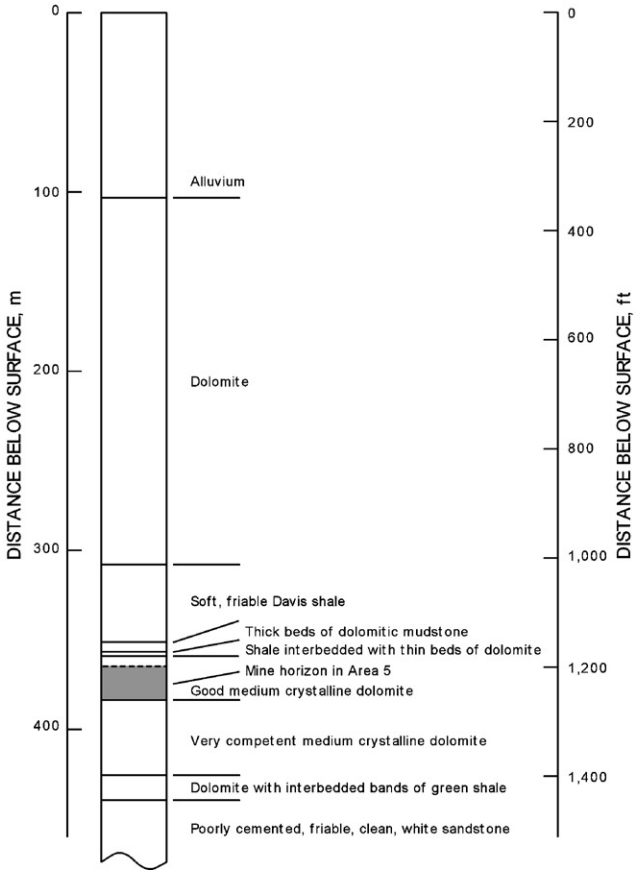

Fig. 2. Generalized stratigraphic column in area 5 (Courtesy of the Doe Run Co.)

with 10-m- (33-ft-) high drifts are now constructed if possible. These larger pillars allow for more efficient backfill operations and provide substantial load-bearing capacity if they are not mined [3].

Secondary mining in the form of pillar extraction is becoming more important as reserves are depleted. Because high-grade support pillars will account for an increasingly larger percentage of future cash flow, successful extraction of these pillars will allow Doe Run to double its remaining mine life. To safeguard the remaining reserves, the backfill plan must ensure that any pillar failures are contained within the backfilled area and do not propagate to adjacent areas, the extent of mine roof failures and accompanying air blasts are limited, and subsidence and breaching of aquifers above mine workings are prevented.

Up to 2 ton (2.2 st) of cemented rockfill per ton of pillar ore is used to extract support pillars in high-grade areas if the unsupported roof span will exceed 46 m (150 ft). Backfill is generally not used in narrow or isolated areas of the mine. Before placement of cemented rockfill begins, the mine roof and pillar ribs are scaled mechanically and manually. Resin-grouted rebar bolts 1.8–2.4 m (6–8 ft) long are then installed to secure the area for backfilling operations. Fill fences consisting of chain-link fence tied to wire rope strung between the pillars are constructed between the pillars to contain the rockfill. As the fenced area is backfilled, horizontal tie-backs are installed for reinforcement. The tie-backs are constructed of 1.2-m- (4-ft-) long No. 7 rebar secured at the end of a 1.3-cm (0.5-in) diam wire rope. The wire rope is looped and clamped around the wire ropes stretched between the pillars. Three anchors located approximately 1.8–3.0 m (5.9–9.8 ft) from the fill fence are installed in each 1-m (3.3-ft), cemented rockfill lift [4].

2. Test area 5

An isolated section of area 5 in the Buick Mine (Fig. 3) measuring 107 × 69 m (350 × 225 ft) was used as a test to prove that the backfill could be used to support the mine roof during pillar extraction and that the mining method was economically feasible, to calibrate a numerical model using data from various instruments installed in the rockfill and the rock mass for planning future pillar mining, and to demonstrate that 100% extraction could be achieved safely.

Pillars were recovered by first backfilling with minus-13-cm (5-in) dolomite waste rock mixed at an underground batching plant with about 4% cement. Wheeled dozers were used to spread the backfill in 0.3- to 0.6-m (1- to 2-ft) lifts to within 3 m (10 ft) of the roof, after which front-end loaders placed the next 2 m (7 ft) of backfill [5]. The final 1-m (3-ft) gap was filled with minus-5-cm (2-in) cemented waste rock with a slinger truck. Because this was the first section in which backfill was used, the fill fence was reinforced with steel and shotcrete.

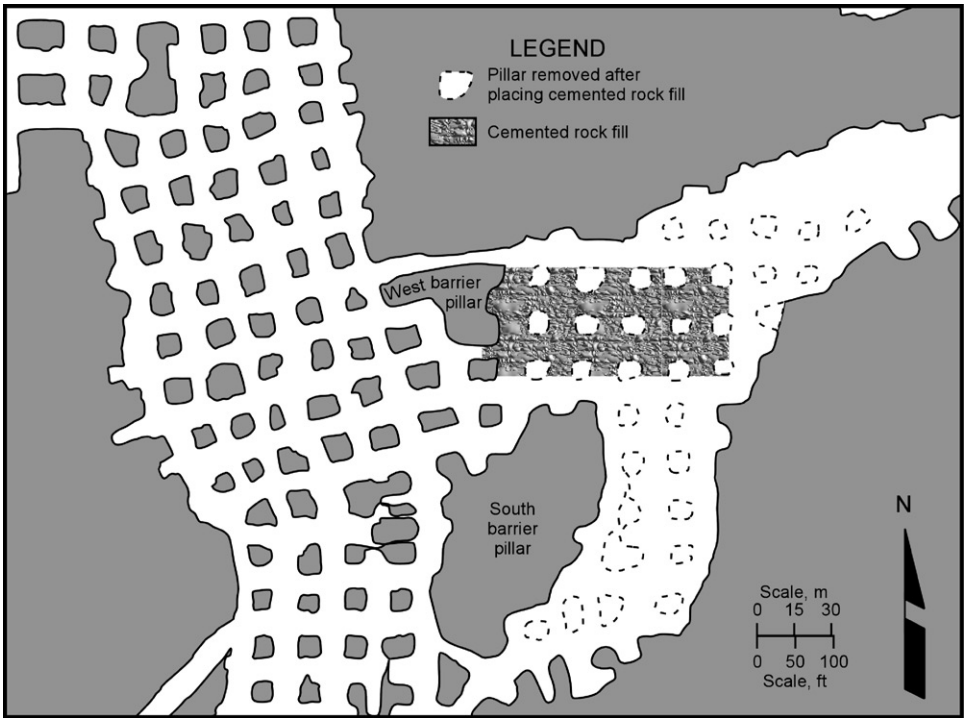

Fig. 3. Plan view of area 5.

Table 1
Pillar extraction sequence, elapsed time in days

Pillar	Day	Pillar	Day
97, east half	0	5, south half	177
96	17	14, north half	177
87, south half	17	112	192
97, west half	17	4, north half	192
95	52	4, south half	199
86, south half	52	13, north half	199
94	59	111	212
105	85	110	212
106	85	93	221
114	101	92	233
5, north half	123	101	389
113, bottom 12.5 m	123	102, 7 holes	444
6, west 3.7 m	123	102, 20 holes	451
113, top 4.3 m	127	104	515
		103	695

2.1. Mining sequence

Pillar extraction proceeded generally from northeast to southwest (Table 1). Perimeter pillars (partially confined pillars) were extracted before the trapped pillars (“trapped” pillars are pillars completely surrounded with backfill) (Fig. 4). The four trapped pillars were drilled and blasted from an access drift approximately 6 m (20 ft) below the test area.

2.2. Instruments and monitoring

Instruments were installed in the backfill, mine roof, pillars, barrier pillars, and abutments (Fig. 4). When the cemented backfill was mid-height to the pillars, it became a working platform for installing horizontal extensometers and biaxial stressmeters in the support pillars. Earth pressure cells and embedment strain gauges were placed in the backfill at this level to measure stress and strain changes. Four vertical extensometers were installed in the mine roof to measure roof sag and strata separation. Earth pressure cells and one embedment strain gauge were placed at the top of the backfill in the two east–west backfilled drifts near three of the extensometers to verify the amount of roof sag and measure load applied to the backfill by the mine roof.

Borehole extensometers were installed in the exterior side of the perimeter pillars at an inclination of 50° up from horizontal. Additional vertical extensometers were placed in the trapped pillars from the sublevel access drift beneath area 5. The borehole extensometers were installed in B-size diamond drillholes with a shallow, large-diameter hole counterbored at the collar to recess the anchor and protect the transducers from equipment and flyrock. The collar anchors for the extensometers in the trapped pillars were placed in the roof of the sublevel access drift, and the two uphole anchors were located approximately at the top and bottom of the trapped pillars.

Fiberglass rods connected the downhole anchors to the transducers at the collar anchor. Copper bladder anchors inflated with hydraulic oil to a pressure of about 9.5 MPa (1400 psi) secured the instruments in the borehole. Data from the extensometers installed in the trapped pillars were used for numerical code calibration.

The embedment strain gauges were 25.4 cm (10 in) long with 5-cm- (2-in-) diam steel flanges at each end. A steel wire-and-spring assembly is tensioned between the flanges in a 2.54-cm- (1-in-) diam PVC tube and provided up to 0.64 cm (0.25 in) of displacement between the flanges. The 23-cm- (9-in-) diam earth pressure cells had a maximum load capacity of 6.9 MPa (1000 psi). Prior to installing the backfill instruments, they were cast in wood forms using minus-0.64-cm- (0.25-in-) cemented aggregate and left to cure for several weeks. The forms were removed before the instruments were secured in place in the test area with wet backfill. To measure average backfill strain, three 4.2-, 11.9-, and 16.5-m- (13.8-, 39.0-, and 54.1-ft-) long vertical fill extensometers were assembled at selected locations in the east–west drifts as the backfill was placed.

To measure the redistribution of stress during pillar extraction, biaxial stressmeters were installed in pillars 102 and 103, the north abutment, and the west and south barrier pillars. These instruments measure radial deformation of a borehole with three vibrating-wire sensors extending across the diameter of a thick-walled steel cylinder. These sensors are oriented 0°, 60°, and 120° from vertical. Secondary principal stress change and direction can be calculated as a frequency change in each of the wires [6,7]. The stressmeter can be equipped with an extra set of radial sensors for backup measurements, as well as two temperature sensors and two longitudinal sensors for additional accuracy. Deformation in the rock is transferred to the stressmeter through a high-strength, nonshrinking grout pumped into a slightly downward-dipping borehole where the instrument is temporarily secured with snap rings activated by a cable at the borehole collar. Data from the biaxial stressmeters and vertical extensometers in the pillars were intended to create an in situ stress-versus-strain plot, but the biaxial stressmeter data were difficult to evaluate as a result of problems with the data acquisition software. Readings for all instruments were automatically recorded every 2 h during removal of the secondary pillars.

Cables were strung through steel pipes placed in the backfill from the instruments to three Campbell Scientific[1] dataloggers [8] on the southwest side of the

[1] Mention of specific products or manufacturers does not imply endorsement by the National Institute for Occupational Safety and Health.

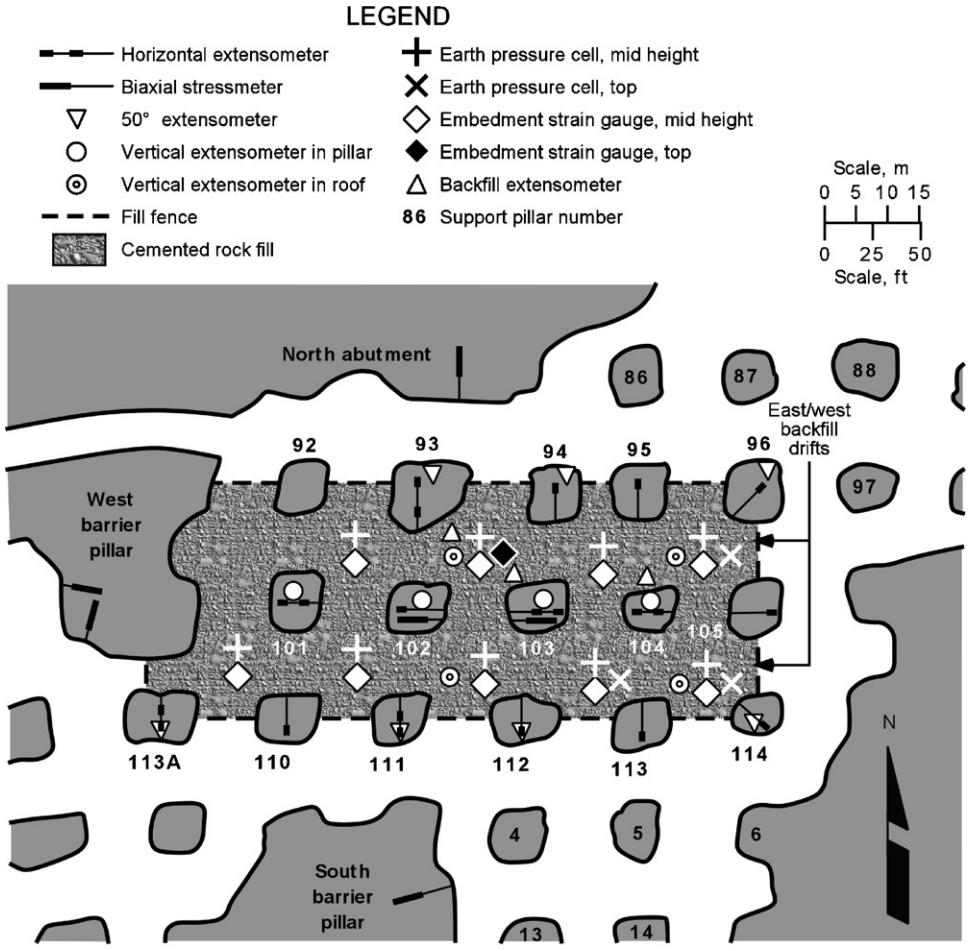

Fig. 4. Plan view of area 5 with instrument locations.

barrier pillar at the west end of area 5. A slot cut with a cutting torch along the pipes' longitudinal axes facilitated cable placement in the pipe and used ventilation fabric kept rockfill out of the slots. A larger diameter pipe cut in half served as a protective cover for the cable at the open joints between the slotted pipes. Backfill was placed to a depth of about 0.5 m (1.6 ft) over the pipes and allowed to cure for 1 day before heavy machinery was driven over it.

Previous analyses of the instrument data along with results from numerical codes indicated that the mine roof, backfill, and perimeter pillars remained stable during the entire pillar extraction sequence [5,9]. However, measured change in elastic vertical strain for trapped pillar 103 greatly exceeded model-calculated strain change when two adjacent pillars were mined, indicating that pillar 103 failed at least partially (Fig. 5). This condition did not present any hazard to miners because the pillars were totally confined.

Manual readings from instruments in the backfill, mine roof, and a support pillar adjacent to the backfilled area were periodically recorded after all the pillars in the immediate test area were mined. These readings indicated that the mine roof loaded the backfill when eight additional support pillars south of the test area were mined 3 years after the test project was completed. Removal of these pillars increased the roof span supported by cemented backfill from 130 to 180 m (427 to 591 ft) [10].

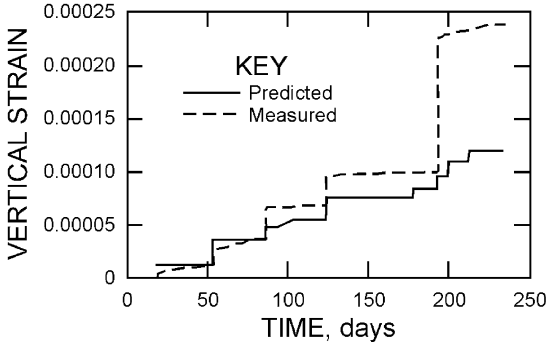

Fig. 5. Measured vertical strain versus time for pillar 103 compared to vertical strain versus time using elastic material properties in a boundary-element numerical model.

3. Numerical modeling

3.1. Geological model and laboratory properties

A three-dimensional, finite-element program, UTAH3, was used to estimate rock mass strength and modulus of deformation and to analyze the effect of support pillar mining on trapped pillars 103 and 104. A continuum model was chosen because area 5 did not contain major faults that could dominate material behavior. It was assumed that rock softening caused by the joint sets and small voids could be reasonably modeled by reducing the modulus of deformation from its laboratory value.

The yield criterion in UTAH3 is Drucker-Prager, in which strength is dependent on all three principal stresses, and the associate flow rules are applied for determining strains in yielded elements. Model concepts are discussed in the two-dimensional version of this code [11]. This code and failure criterion have been successfully used in US Bureau of Mines and NIOSH research projects at the Homestake Mine in Lead, SD, USA [12].

Because the pillars were confined by backfill and the backfill was filled tight to the mine roof, elastic perfectly plastic behavior for the rock was assumed. This material model was also chosen for the rockfill because it was assumed that the large volume of material would provide self-confinement if it failed.

Since this research was conducted, stress-versus-strain plots have been produced from triaxial tests performed by researchers at the University of New South Wales and Fosroc Chemfix on specimens composed of minus-50-mm (2-in) dolerite with 7.2% cement content and a 2:1 water-to-cement ratio. These tests confirmed that the specimens were ductile and that the stress-versus-strain relationship can be idealized with an elastic perfectly plastic material model [13].

The finite-element mesh contained 252,000 elements representing a rock mass $271 \times 271 \times 535$ m ($890 \times 890 \times 1755$ ft) with a 18.3-m- (60-ft-) thick mining horizon 366 m (1200 ft) below the surface and 151 m (495 ft) above the bottom of the rock mass block. Rollered boundary conditions were used on all sides of the block except the top, which was free to move vertically. Cubes 4.6 m (15 ft) on a side simulated the rock mass from 9 m (30 ft) below to 46 m (150 ft) above the mining horizon. The remaining elements were $4.6 \times 4.6 \times 9.1$ m ($15 \times 15 \times 30$ ft) and formed "bricks" with the longest dimension along the vertical axis. Rooms and pillars were formed using multiple "bricks" that best matched the actual geometry, but the node coordinates for pillars 93, 102, 103, and 104 were adjusted to conform to the pillar boundaries more accurately.

Model stratigraphy was based on a generalized stratigraphic column supplied by Doe Run (Fig. 2), and boundaries between rock types were adjusted to coincide with the nearest vertical coordinate in the mesh. In the initial computer run, material property values for dolomite were obtained from specimens tested at the Spokane Research Laboratory (SRL). The specific weight for dolomite was obtained by averaging the weight of BX core specimens from the abutment north of area 5, the west barrier pillar, and the barrier pillar west of pillar 4. Dolomitic mudstone and shale property values were based on published laboratory tests [14]. Elastic material property values for the cemented rockfill were calculated from in situ measurements, and strength values were estimated from laboratory tests conducted with similar cemented backfill specimens [15] (Table 2). Values in the calibrated model were reduced to account for rock fractures and other discontinuities.

The ratio of horizontal to vertical in situ stresses used in the model was the same as the ratio obtained from three-dimensional in situ stress measurements in an abutment in the north part of the Buick Mine (Tables 3,4) [16]. Four hollow inclusion stress cells manufactured by Australia's Commonwealth Scientific and Industrial Research Organization (CSIRO) were set and overcored at depths between 13.4 and 16.5 m (44 and 54 ft). This area was a room-and-pillar section approximately 72 m (235 ft) wide and 305 m (1000 ft) deep with cube-shaped pillars measuring 7.6 m (25 ft) on each side; rooms were 10.7 m (35 ft) wide [16].

After applying in situ stresses to the elements in the model, researchers mined the rooms, sublevel haulage drifts, the majority of the pillars northeast of the test area, and a sublevel access drift to area 5. Because the rock at the mining horizon was represented by cubes with 4.6-m (15-ft) sides, the heights of the excavated areas were modeled to the nearest 4.6 m (15 ft). Next, area 5 was backfilled and the support pillars were mined.

3.2. Deformation modulus

The numerical model was used to estimate rock mass modulus by plotting changes in elastic vertical strain measured in the trapped pillars as the independent variable and UTAH3-calculated vertical strain change as the dependent variable (Fig. 6). Plots of cumulative vertical strain versus time were also used.

The model was run with incrementally smaller rock modulus and strength values until, on day 192, some of the elements in pillar 103 failed, and a slope of approximately 1.0 was calculated using regression analyses on the strain data. Strain data for pillar 104 were not used after day 17 because the model predicted partial failure of this pillar after this day with the excavation of pillars 95 and 86. The same value for pre- and post-failure deformation modulus was used in each computer run. With a deformation modulus equal to 37,232 MPa (5,400,000 psi), or approximately 45% of

Table 2
Summary of average laboratory properties

	Young's modulus		Unconfined compressive strength		Tensile strength		Specific weight		Poisson's ratio
	MPa	psi	Mpa	psi	MPa	psi	kg/m^3	Lb/ft^3	
Dolomite	84830.0	12,303,550	108.9	15,800	10.9	1580	2563	160	0.26
Dolomitic mudstone	34480.0	5,000,900	54.0	7830	5.4	780	2563	160	0.25
Shale	17240.1	2,500,460	54.0	7830	5.4	780	2195	137	0.25
Cemented backfill	1909.8	277,000	6.9	1000	0.7	100	2114	132	0.30

Table 3
Major principal stresses

Stress[a]		Azimuth (deg)[b]	Dip (deg)[c]
MPa	psi		
24.52	3557	239.6	1.6
7.98	1157	127.7	85.8
3.44	499	149	−3.9

[a] Positive sign indicates compressive stress.
[b] Angle clockwise from north is positive.
[c] Angle down from horizontal is positive.

Table 4
Cartesian stresses

Type of stress	Direction	Amount	
		MPa	psi
Normal	North–south	8.86	1285
Normal	East–west	19.12	2773
Normal	Vertical	7.97	1156
Shear	North–south, east–west	9.19	1333
Shear	East–west, vertical	−0.23	−34
Shear	Vertical, north–south	−0.50	−72

the laboratory deformation modulus, and a rock mass strength of 43 MPa (6200 psi), representing approximately 40% of the unconfined compressive strength, the slope of the regression line for the measured-versus-calculated strain data was 0.85 (Fig. 6), indicating that the modulus could be reduced an additional 15%. However, decreasing the modulus would cause the cumulative calculated strain to further exceed the measured cumulative strain in pillars 103 and 104 (Figs. 7 and 8). When the modulus was increased to 60% of its laboratory value, cumulative calculated strain traced measured strain reasonably well for pillars 103 and 104. Based on these results, an estimate for the in situ rock mass deformation modulus ranged from 45% to 60% of the laboratory value.

Some data scatter can be attributed to the large amount of calculated (versus measured) vertical strain on pillar 103 when pillar 94 was mined on day 59 (Figs. 6 and 7) A possible explanation is that pillar 94 softened when adjacent pillar 95 and the south end of pillar 86 were mined, and this softening was then manifested in a larger creep rate after day 52 (Fig. 9).

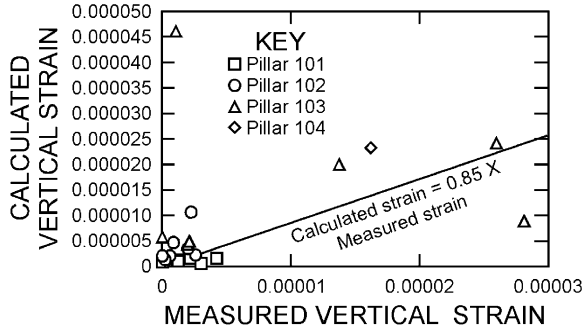

Fig. 6. Measured versus model-calculated strain in trapped pillars.

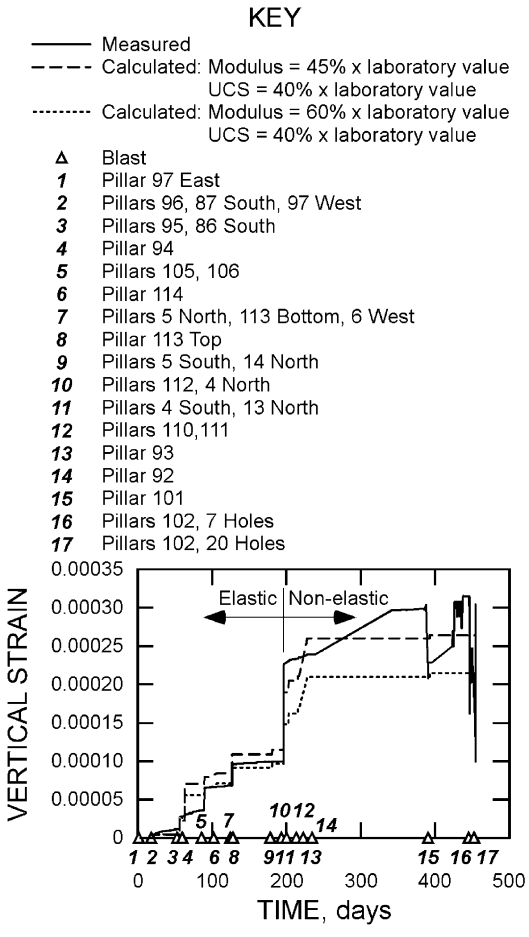

Fig. 7. Vertical strain versus time for pillar 103.

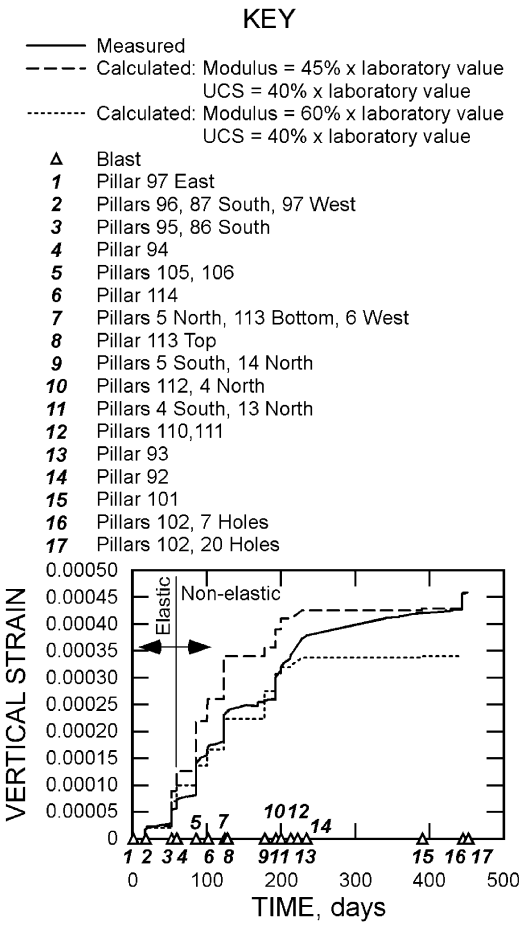

Fig. 8. Vertical strain versus time for pillar 104.

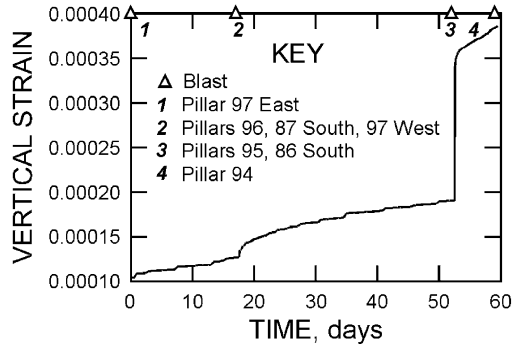

Fig. 9. Vertical strain versus time for pillar 94.

Visual observations confirm that the pillar was damaged after pillars 95 and 86 were mined.

A rock mass rating (RMR) was also used to calculate a modulus reduction factor (Table 5) [17]. Approximately 15 m (50 ft) of BX-size core recovered from the west barrier pillar was used to calculate the rock quality designation (RQD). Using the equation for in situ rock mass modulus of deformation (E_M), in which [18]

$$E_M = 2 \times \mathrm{RMR} - 100, \quad (1)$$

yields an in situ rock mass modulus equal to 44 GPa (6,381,660 psi), or 52% of the laboratory modulus of deformation.

Table 5
RMR parameters and their values for area 5

Parameter	Value or description	RMR value
Unconfined compressive strength	109 MPa (15,800 psi)	12
RQD	95	20
Spacing of joints	0.13–1 m	10[a]
Condition of joints	Slightly rough surfaces Separation <1 mm Hard joint wall rock	20
Groundwater	Dry	10
Total		72

[a] Conservatively chosen because of closely spaced joints (0.13 m) in some areas.

3.3. Pillar strength

The trapped pillars could not be directly observed because they were confined by cemented rockfill; however, data from the vertical extensometer installed in pillar 103 and results from elastic modeling [5] suggest that this pillar failed for the following reasons.

1. The model-calculated change in elastic vertical strain for pillar 103 caused by mining pillars 112 and 4 was nine times smaller than the measured strain change, indicating that the pillar was probably not behaving elastically after day 192 (Fig. 5).
2. When blast holes were being drilled in pillar 103 from the sublevel access drift, the operator reported that the drill steel jammed. This problem is commonly encountered in broken ground.
3. When pillar 93 was mined, the measured change in vertical strain for pillar 103 was very small compared with the vertical strain change in pillar 101, even though pillar 93 was approximately equidistant from pillars 101 and 103. If pillar 103 were still behaving elastically, the expected strain would be comparable to that of pillar 101 (Fig. 10).
4. After day 385, the displacement readings corresponding to the extensometer anchor installed near the top of pillar 103 were erratic, as indicated by the vertical strain plot (Fig. 7). This behavior could be attributed to an anchor loosening as a result of pillar failure near the mine roof.
5. The earth pressure cells installed in the north backfill drift measured stress increases when pillars 110, 111, and 93 were mined (Fig. 11), but the vertical extensometer in pillar 103 did not measure significant increases in vertical strain (Fig. 7). Because the

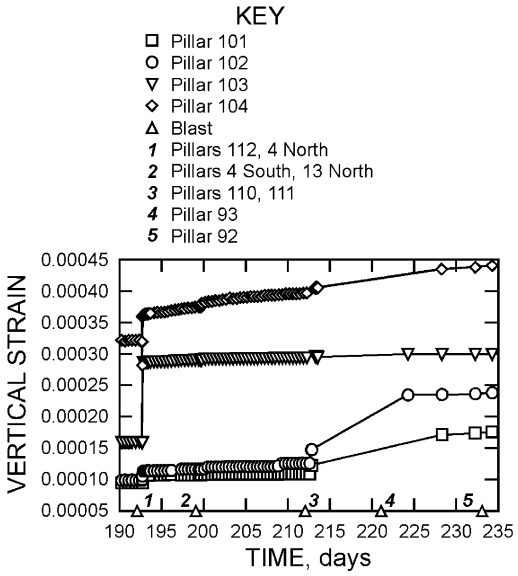

Fig. 10. Vertical strain versus time for pillars 101, 102, 103, and 104.

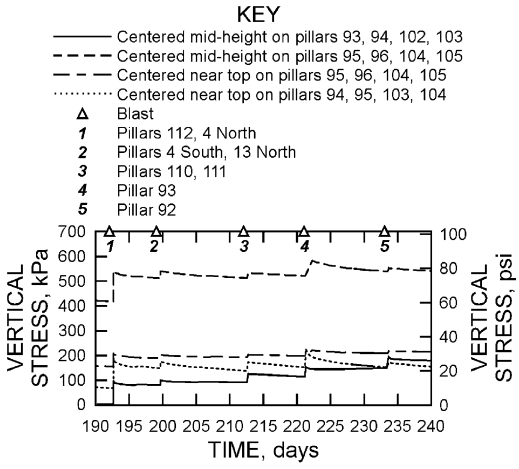

Fig. 11. Vertical stress versus time for earth pressure cells in the northern east–west backfill drift.

backfill has a much lower modulus of deformation than the host rock, an intact rock pillar should have exhibited significant increases in strain as a result of these redistributed loads.

6. After the adjacent perimeter pillar 112 was mined on day 192, most of the measured vertical strain in pillar 103 was time dependent. The negligible response of pillar 103 to subsequent extraction of other pillars in the vicinity indicated that the pillar had softened substantially.

With a deformation modulus between 37,232 and 49,815 MPa (5,400,000 and 7,225,000 psi) and a rock mass unconfined compressive strength equal to 43 MPa (6200 psi), or 40% of the laboratory unconfined compressive strength value, UTAH3 calculated that 50% of the elements in the center of pillar 103 would fail when pillars 112 and 4 were mined. Because some of the pillar elements remained elastic, the average vertical stress in the pillar was 47.6 MPa (6909 psi). The model calculated failure in the center of pillar 104 when pillars 95 and 86 were mined. This earlier failure is consistent with the high strain measured in pillar 104 as compared to strain in pillar 103. No additional elements in pillar 104 failed as mining progressed.

The Hoek–Brown generalized failure criterion for jointed rock [19] was also used to estimate pillar strength. This formula is

$$\sigma_1' = \sigma_3' + \sigma_{ci}(m_b\sigma_3'/\sigma_{ci} + s)^a, \quad (2)$$

where σ_1' and σ_3' are the maximum and minimum effective stresses at failure, m_b the value of the Hoek-Brown constant m for the rock mass, s and a the constants that depend upon rock mass characteristics and σ_{ci} the uniaxial compressive strength of intact rock.

For an estimate of the unconfined compressive strength for the rock mass, Eq. (2) reduces to Eq. (3), so that

$$\sigma_1' = \sigma_{ci}s^a \quad (3)$$

and

$$s = \exp((GSI - 100)/9). \quad (4)$$

GSI is the geological strength index developed by Hoek [20] and Hoek et al. [21] to estimate the reduction in rock mass strength for different geological conditions. It is presented in tabular form in [22]. Based on the existence of two joint sets and one set of bedding planes in area 5, the GSI value is estimated as 80. For a GSI value greater than 25, a is equal to 0.5. Using Eqs. (3) and (4), the reduction factor in rock mass strength (s^a) for a GSI value of 80 equals 0.33. This value agrees reasonably well with 0.4 determined from the numerical model.

Pillar stress at failure was estimated using the relationship between pillar stress and height for unconfined pillars [3]. This relationship was established by combining a visual rating system to quantify pillar condition and a displacement discontinuity numerical model to calculate vertical stress in those pillars. Pillars were assigned a number from 1 to 6, where 1 represents a pillar with no visual fractures and 6 represents a failed pillar (Table 6) (Fig. 12). A similar method was also applied at Boliden Mineral AB's Black Angel Mine in Marmorik, Greenland, and Laisvall Mine in northern Sweden [23,24].

The ratio of pillar stress to unconfined compressive strength was plotted as a function of pillar height for each pillar rating number (Fig. 13). This empirical curve was developed from data collected over the last decade. For a pillar height of 18.3 m (60 ft) and a pillar rating equal to 6, the ratio of pillar load to unconfined compressive strength is approximately 0.23. For a

Table 6
Pillar condition rating system (after [3])

Pillar rating	Pillar condition
1	No indication of stress-induced fracturing. Intact pillar.
2	Spalling on pillar corners, minor spalling of pillar walls. Fractures oriented subparallel to walls and are short relative to pillar height.
3	Increased corner spalling. Fractures on pillar walls more numerous and continuous. Fractures oriented subparallel to pillar walls, and lengths are less than half pillar height.
4	Continuous, subparallel, open fractures along pillar walls. Early development of diagonal fractures (start of hourglassing). Fracture lengths are greater than half pillar height.
5	Continuous, subparallel, open fractures along pillar walls. Well-developed diagonal fractures (classic hourglassing). Fracture lengths are greater than half pillar height.
6	Failed pillar, may have residual load-carrying capacity and be providing local support to stope back. Extreme hourglass shape or major blocks fallen.

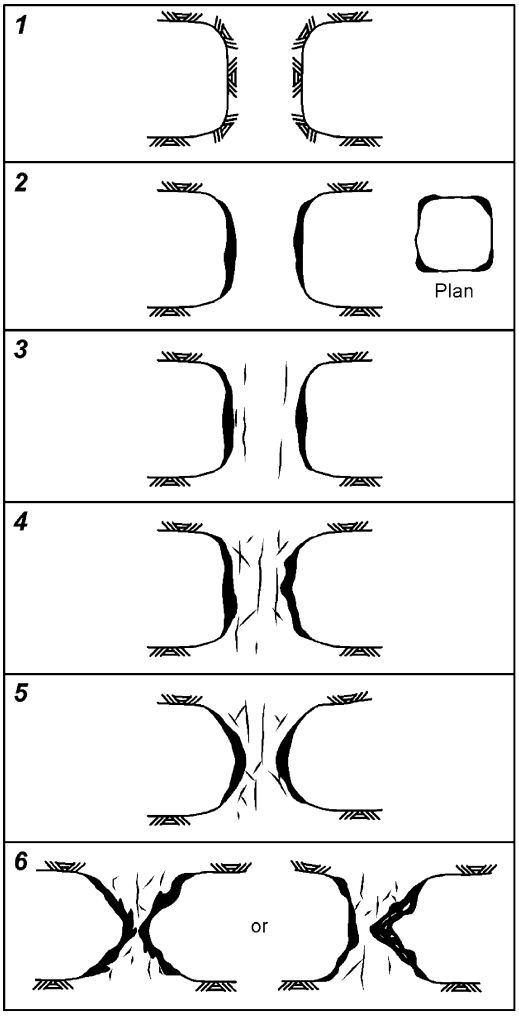

Fig. 12. Pillar condition rating system.

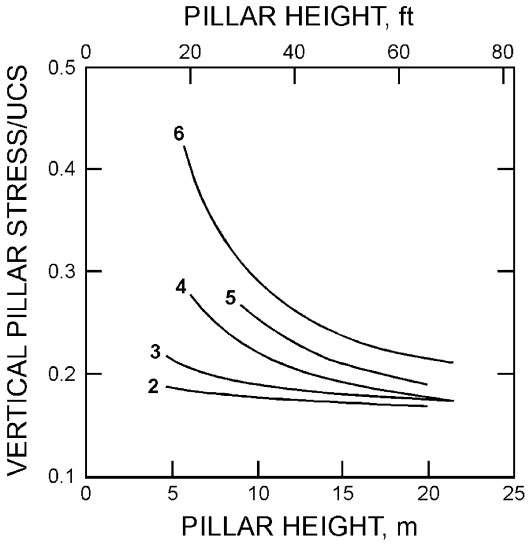

Fig. 13. Pillar height versus vertical pillar stress for all Doe Run mines (after [3]).

unconfined compressive strength equal to 148.2 MPa (21,500 psi), an average for pillars in all of Doe Run's mines, the calculated pillar stress in a failed state is 34.1 MPa (4945 psi). The larger stress of 47.6 MPa (6909 psi) calculated by UTAH3 may be attributed to the ability of the elastic elements in the pillar to carry more load than the failed elements.

Furthermore, a confined pillar should be able to support more load than an unconfined pillar. The effect of confinement on stress was observed at Cyprus Twentymile Coal Co.'s Foidel Creek Mine near Oak Creek, CO. Three parallel 6-m- (20-ft-) wide entries were driven across a 248-m- (815-ft-) wide longwall panel to provide access for development of gateroad entries and escapeways for underground miners. Biaxial stress-meters and horizontal extensometers were installed in the cross-panel support pillars and the rib of the longwall panel to measure stress changes as well as pillar and rib dilation as the longwall face advanced. After the gateroad entries were developed, the cross-panel entries were backfilled with an air-entrained mixture of flyash and cement, fully confining the in-panel support pillars. When the panel rib dilated 1.3 cm (0.5 in), the major secondary principal stress change was

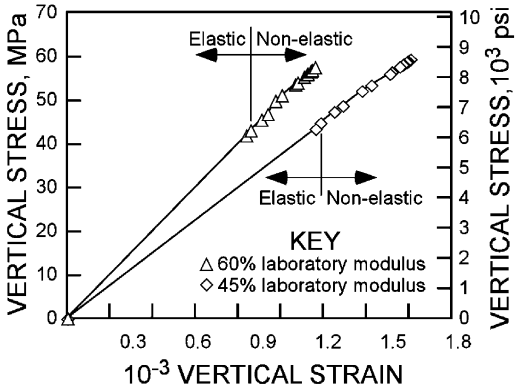

Fig. 14. Vertical stress versus vertical strain for pillar 104 produced using an elastic–plastic material model.

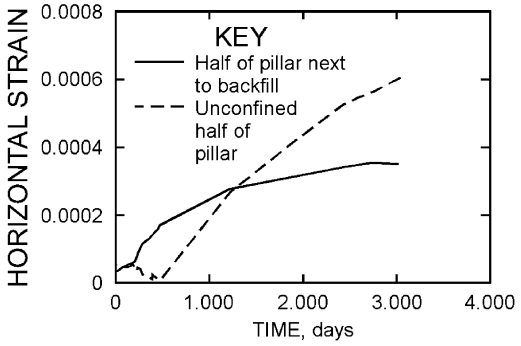

Fig. 15. Horizontal strain versus time for pillar 113A.

about 1.52 MPa (220 psi), whereas the stress change in the confined cross-panel entry pillar was 7.14 MPa (1035 psi) for the same amount of dilation [25].

Pillar confinement and partial failure (versus total failure) may also explain why UTAH3 calculated increases in average post-failure vertical stress for pillars 103 and 104 as more pillars were mined, resulting in a strain-hardening stress-versus-strain plot (Fig. 14). Although stress measurements were not obtained for these two pillars, there is evidence that backfill confinement limited pillar dilation. Strain measurements obtained from a horizontal extensometer installed in perimeter pillar 113A (Fig. 4) indicated that the unconfined south side of this pillar underwent more strain than the north side, which was confined with backfill (Fig. 15).

4. Conclusions

Data from vertical extensometers installed in support pillars confined by cemented rockfill at the Buick Mine indicated that these pillars failed or partially failed when other nearby support pillars were mined. This was corroborated by drill operators when the drill steel bound in the drill holes as the pillars were prepared for blasting.

Extensometer data indicated that there was immediate compressive strain in response to nearby mining, followed by time-dependent strain. At some point after failure, the extensometers in one failed pillar did not record any immediate response to additional mining, and strain became nearly 100% time dependent.

An elastic perfectly plastic material model applied in a calibrated three-dimensional, finite-element numerical model adequately traces pre- and post-failure strain-versus-time for two backfill-confined pillars. A strain-hardening, post-failure stress-versus-strain plot was also produced. Post-failure stresses calculated by the finite-element model were larger for confined pillars than post-failure stresses in unconfined pillars calculated with empirical plots. Because a better understanding of the loading capabilities of support pillars is critical to designing a safe and economic mine, additional research is merited.

Rock mass modulus values equal to 45–60% of laboratory values were used in a calibrated three-dimensional, finite-element program to account for softening caused by the interaction of joint sets. The range in the modulus estimate was necessary because a plot of measured versus model-calculated strain resulted in scattered data. An empirical correlation between RMR and rock mass modulus yielded a rock mass modulus equal to 52% of the laboratory deformation modulus.

Similarly, a reduced unconfined compressive strength of 43 MPa (6200 psi), or approximately 40% of the average unconfined compressive strength obtained from laboratory tests, was used in the calibrated numerical model to account for fractures in the rock mass. The Hoek–Brown failure criterion for strength in a jointed rock mass yielded a reduction equal to 33% of average laboratory unconfined compressive strengths.

Complementary instruments installed in the cemented backfill and support pillars were used to identify pillar behavior. For example, stress increases in earth pressure cells combined with little or no movement measured by vertical extensometers installed in the pillars helped confirm that the pillars were softening.

Acknowledgements

The authors wish to express their appreciation to the management of The Doe Run Co., Buick Mine, St. Louis, MO, and especially to Bill Lane, manager-Mine Technical Services, for assisting in the development of the instrumentation plan, providing access to the test section in the mine, supplying and maintaining instruments and data acquisition systems, and providing mine maps and schedules. Other people who provided much assistance were Lyndon Clark, senior engineer, The Doe Run Co., who gave us information on mining practices

and suggested improvements in modeling techniques; William Pariseau, professor, Department of Mining Engineering, University of Utah, Salt Lake City, UT, who modified UTAH3 to accommodate backfill cycles; and Jeff Johnson, mining engineer, SRL, who wrote the UTAH3 mesh generator and assisted with interpretations of UTAH3 model results.

References

[1] National Research Council, Committee on Technology for the Mining Industries. Evolutionary and revolutionary technologies for mining. Washington, DC: National Academy Press, 2001. p. 47.

[2] Agapito JFT, Goodrich RR. Pre-failure pillar yielding. Presentation, SME Annual Meeting, 2001. 12pp.

[3] Roberts DP, Lane WL, Yanske TR. Pillar extraction at the Doe Run Company 1991 to 1998. In: Bloss M, editor. Proceedings of the Sixth International Symposium on Mining with Backfill, Victoria: Australian Institute of Mining and Metallurgy, 1998. p. 227–33.

[4] Yanske TR, Clark LM, Carmack JE, CRF pillar construction at the Doe Run Company. In: Stone D, editor. Minefill 2001: Proceedings of the Seventh International Symposium on Mining with Backfill, Colorado: The Society for Mining Metallurgy and Exploration Inc., 2001. p. 337–49.

[5] Tesarik DR, Seymour JB, Yanske TR, McKibbin RW. Stability analysis of a backfilled room-and-pillar mine. US Bur Mines Rep Invest 9565, 1995, 20pp.

[6] McRae JB, Simmonds T. Long-term stability of vibrating wire instruments: one manufacturer's perspective. In: Sorum G, editor. Proceedings: Third International Symposium on Field Measurements in Geomechanics, Rotterdam: A.A. Balkema, 1991. p. 283–93.

[7] Seymour JB, Tesarik DR, McKibbin RW, Jones FM. Monitoring mining-induced stress changes with the biaxial stressmeter. In: Leung CF, Tan SA, Phoon KK, editors. Field measurements in geomechanics. Proceedings of the Fifth International Symposium on Field Measurements in Geomechanics, Rotterdam: A.A. Balkema, 1999. p. 55–60.

[8] Larson MK, Tesarik DR, Seymour JB, Rains RL. Instruments for monitoring stability of underground openings. In: Mark C, Dolinar DR, Tuchman R, Barzak TM, Signer SP, Wopat PF, editors. Proceedings of the New Technology for Coal Mine Roof Support. US Bur Mines Inform Cir 9453, 2000. p. 253–69.

[9] Lane WL, Yanske TR, Roberts DP. Pillar extraction and rock mechanics at the Doe Run Company in Missouri 1991 to 1999. In: Amadei B, Kranz RL, Scott GA, Smeallie PH, editors. Rock Mechanics for Industry: Proceedings of the 37th US Rock Mechanics Symposium, Rotterdam: A.A. Balkema, 1999. p. 285–92.

[10] Tesarik DR, Seymour JB, Yanske TR. Long-term stability of a backfilled room-and-pillar mine. In: Leung CF, Tan SA, Phoon KK, editors. Field Measurements in Geomechanics. Proceedings of the Fifth International Symposium on Field Measurements in Geomechanics, Rotterdam: A.A. Balkema, 1999. p. 431–5.

[11] Pariseau WG. Interpretation of rock mechanics data (contract HO220077 Univ of UT). US Bur Mines OFR-47(2)-80, vol. 2, 1978. 41pp.

[12] Pariseau WG, Duan F, Schmuck CS. Stability analysis of the VCR stope at the Homestake Mine. Gold Min 1987;87:199–213.

[13] Sainsbury D, Yuejun C, Thompson B. Investigation of the geomechanical characteristics of stabilized rockfill. In: Stone D, editor. Minefill 2001: Proceedings of the Seventh International Symposium on Mining with Backfill, Colorado: The Society for Mining Metallurgy and Exploration Inc., 2001. p. 105–15.

[14] Farmer IW. Engineering properties of rocks. London: Butler and Tanner, 1968. 180pp.

[15] Tesarik DR, Vickery JD, Seymour JB. Evaluation of in situ cemented backfill performance. US Bur Mines Rep Invest 9360, 1991. 26pp.

[16] Tesarik DR, McKibbin RW. Instrumentation and modeling of the north 140 section of Magmont Mine, Bixby, MO. US Bur Mines Rep Invest 9215, 1989. 30pp.

[17] Hoek E, Brown ET. Underground excavations in rock. London: the institution of mining and metallurgy, 1980. p. 22–7.

[18] Bieniawski ZT. Rock mechanics in mining and tunneling. Rotterdam: Balkema, 1984. p. 79–80.

[19] Hustrulid WA, Bullock BL, editors. Underground mining methods. Littleton, CO: Soc Min, Metall, and Explor Eng, 2001.

[20] Hoek E. Strength of rock and rock masses. Int Soc Rock Mech News J 1994;2(2):4–16.

[21] Hoek E, Kaiser PK, Bawden WF. Support of underground excavations in hard rock. Rotterdam: Balkema, 1995. 215pp.

[22] Hoek E, Marinos P, Benissi M. Applicability of the geological strength index (GSI) classification for weak and sheared rock masses: the case of the Athens schist formation. Bull Eng Geol Environ 57(2):151–60.

[23] Krauland N, Soder P. Determining pillar strength for pillar failure observation. Eng Min J 1987;188(8):34–40.

[24] Soder P, Krauland N. Determination of pillar strength by full-scale pillar tests in the Laisvall Mine. In: Kidybinski, Dubinski, editors. Proceedings: Proceedings of the 11th Plenary Scientific Session of the International Bureau of Stratamechanics; Strata Control in Deep Mines, Colorado: The Society for Mining Metallurgy and Exploration Inc., 1990. p. 39–59.

[25] Seymour JB, Tesarik DR, Larson MK, Shoemaker J. Stability of backfilled cross-panel entries during longwall mining. In: Peng, SS, editor. Proceedings of the 17th International Conference on Ground Control in Mining, Morgantown: University of West Virginia, 1998. p. 11–20.